VERITAS Observations of the BL Lac Object TXS 0506+056

M. Santander – University of Alabama
et al.

Citation of published version:

Abeysekara, A.U., et al. (2018): VERITAS Observations of the BL Lac Object TXS 0506+056. *The Astrophysical Journal Letters*, 861(2).
DOI: https://doi.org/10.3847/2041-8213/aad053

The Astrophysical Journal Letters, 861:L20 (6pp), 2018 July 10 https://doi.org/10.3847/2041-8213/aad053

VERITAS Observations of the BL Lac Object TXS 0506+056

A. U. Abeysekara[1], A. Archer[2], W. Benbow[3], R. Bird[4], A. Brill[5], R. Brose[6,7], J. H. Buckley[2], J. L. Christiansen[8], A. J. Chromey[9], M. K. Daniel[3], A. Falcone[10], Q. Feng[11], J. P. Finley[12], L. Fortson[13], A. Furniss[14], G. H. Gillanders[15], O. Gueta[7], D. Hanna[11], O. Hervet[16], J. Holder[17], G. Hughes[3], T. B. Humensky[5], C. A. Johnson[16], P. Kaaret[18], P. Kar[1], N. Kelley-Hoskins[7], M. Kertzman[19], D. Kieda[1], M. Krause[7], F. Krennrich[9], M. J. Lang[15], P. Moriarty[15], R. Mukherjee[20], S. O'Brien[21], R. A. Ong[4], A. N. Otte[22], N. Park[23,24], A. Petrashyk[5], M. Pohl[6,7], E. Pueschel[7], J. Quinn[21], K. Ragan[11], P. T. Reynolds[25], G. T. Richards[22], E. Roache[3], C. Rulten[13], I. Sadeh[7], M. Santander[26], S. S. Scott[16], G. H. Sembroski[12], K. Shahinyan[13], J. Tyler[11], S. P. Wakely[24], A. Weinstein[9], R. M. Wells[9], P. Wilcox[18], A. Wilhelm[6,7], D. A. Williams[16], T. J Williamson[17], B. Zitzer[11]
(The VERITAS Collaboration), and
A. Kaur[10]
[1] Department of Physics and Astronomy, University of Utah, Salt Lake City, UT 84112, USA
[2] Department of Physics, Washington University, St. Louis, MO 63130, USA
[3] Fred Lawrence Whipple Observatory, Harvard-Smithsonian Center for Astrophysics, Amado, AZ 85645, USA
[4] Department of Physics and Astronomy, University of California, Los Angeles, CA 90095, USA
[5] Physics Department, Columbia University, New York, NY 10027, USA
[6] Institute of Physics and Astronomy, University of Potsdam, D-14476 Potsdam-Golm, Germany
[7] DESY, Platanenallee 6, D-15738 Zeuthen, Germany
[8] Physics Department, California Polytechnic State University, San Luis Obispo, CA 94307, USA
[9] Department of Physics and Astronomy, Iowa State University, Ames, IA 50011, USA
[10] Department of Astronomy and Astrophysics, 525 Davey Lab, Pennsylvania State University, University Park, PA 16802, USA
[11] Physics Department, McGill University, Montreal, QC H3A 2T8, Canada
[12] Department of Physics and Astronomy, Purdue University, West Lafayette, IN 47907, USA
[13] School of Physics and Astronomy, University of Minnesota, Minneapolis, MN 55455, USA
[14] Department of Physics, California State University, East Bay, Hayward, CA 94542, USA
[15] School of Physics, National University of Ireland Galway, University Road, Galway, Ireland
[16] Santa Cruz Institute for Particle Physics and Department of Physics, University of California, Santa Cruz, CA 95064, USA
[17] Department of Physics and Astronomy and the Bartol Research Institute, University of Delaware, Newark, DE 19716, USA
[18] Department of Physics and Astronomy, University of Iowa, Van Allen Hall, Iowa City, IA 52242, USA
[19] Department of Physics and Astronomy, DePauw University, Greencastle, IN 46135-0037, USA
[20] Department of Physics and Astronomy, Barnard College, Columbia University, NY 10027, USA
[21] School of Physics, University College Dublin, Belfield, Dublin 4, Ireland
[22] School of Physics and Center for Relativistic Astrophysics, Georgia Institute of Technology, 837 State Street NW, Atlanta, GA 30332-0430, USA
[23] Wisconsin IceCube Particle Astrophysics Center and Department of Physics, University of Wisconsin-Madison, Madison, WI 53703, USA
[24] Enrico Fermi Institute, University of Chicago, Chicago, IL 60637, USA
[25] Department of Physical Sciences, Cork Institute of Technology, Bishopstown, Cork, Ireland
[26] Department of Physics and Astronomy, University of Alabama, Tuscaloosa, AL 35487, USA; jmsantander@ua.edu
Received 2018 June 7; revised 2018 June 28; accepted 2018 June 29; published 2018 July 12

Abstract

On 2017 September 22, the IceCube Neutrino Observatory reported the detection of the high-energy neutrino event IC 170922A, of potential astrophysical origin. It was soon determined that the neutrino direction was consistent with the location of the gamma-ray blazar TXS 0506+056 (3FGL J0509.4+0541), which was in an elevated gamma-ray emission state as measured by the *Fermi* satellite. Very Energetic Radiation Imaging Telescope Array System (VERITAS) observations of the neutrino/blazar region started on 2017 September 23 in response to the neutrino alert and continued through 2018 February 6. While no significant very-high-energy (VHE; $E > 100$ GeV) emission was observed from the blazar by VERITAS in the two-week period immediately following the IceCube alert, TXS 0506+056 was detected by VERITAS with a significance of 5.8 standard deviations (σ) in the full 35 hr data set. The average photon flux of the source during this period was $(8.9 \pm 1.6) \times 10^{-12}$ cm^{-2} s^{-1}, or 1.6% of the Crab Nebula flux, above an energy threshold of 110 GeV, with a soft spectral index of 4.8 ± 1.3.

Key words: astroparticle physics – BL Lacertae objects: individual (TXS 0506+056, VER J0509+057) – gamma rays: galaxies – quasars: general – neutrinos

1. Introduction

The extragalactic gamma-ray sky is dominated by blazars (Dermer & Giebels 2016; Madejski & Sikora 2016), a subclass of radio-loud active galactic nuclei powered by a central supermassive black hole that displays relativistic jets, with one pointed close to the Earth's line of sight. The spectral energy distributions (SEDs) of blazars are characterized by two broad emission "bumps." The first one, in the radio to X-ray range, is believed to be due to synchrotron emission from relativistic electrons and positrons (henceforth electrons) in the jet. The origin of the second bump, in the X-ray to gamma-ray range, is less clear and is usually attributed in "leptonic" models to the inverse-Compton scattering of low-energy photons by electrons in the jet, and in "hadronic" models to proton synchrotron, or to

the decay of high-energy mesons produced in cosmic-ray interactions. See Böttcher et al. (2013) and references therein for a recent summary of leptonic and hadronic modeling of blazar SEDs.

The potential hadronic origin of the high-energy emission from blazars (Mannheim 1993) makes them candidate neutrino sources (Mannheim 1995; Halzen & Zas 1997) and, as such, they have been suggested as the origin of the astrophysical neutrino flux detected by the IceCube observatory at energies between ∼20 TeV and a few PeV (IceCube Collaboration 2013). While the isotropic distribution of the IceCube astrophysical neutrinos favors an extragalactic origin, the source of the flux remains unknown and no significant correlation has been found in studies that involve neutrino positions and blazars detected by the *Fermi*-Large Area Telescope (LAT) gamma-ray space telescope (Aartsen et al. 2017), constraining the fractional contribution from *Fermi*-LAT blazars to the all-sky astrophysical neutrino flux to be lower than 27%. While the IceCube measurement excludes *Fermi*-LAT blazars as the main source of the neutrino flux, the constraint has important caveats as it depends on the assumed neutrino flux spectrum, and the variability and other intrinsic characteristics of the sources considered. Therefore, it does not exclude the identification of an individual blazar as a potential neutrino counterpart.

In 2016 IceCube started broadcasting real-time alerts for astrophysical neutrino candidate events to enable prompt follow-up observations that could identify electromagnetic counterparts to the astrophysical neutrinos. These alerts are issued by the Astrophysical Multimessenger Observatory Network (Smith et al. 2013) and are circulated using the Gamma-ray Coordinates Network (GCN).[27]

On 2017 September 22, IceCube reported the detection of a high-energy astrophysical neutrino candidate event, IC 170922A.[28] The initial reconstructed direction of the neutrino (Kopper & Blaufuss 2017) was consistent with that of the gamma-ray blazar TXS 0506+056, which was observed to be in a high gamma-ray emission state by *Fermi*-LAT (Tanaka et al. 2017). Follow-up observations of the neutrino/blazar position led to the first detection of this blazar in the VHE range by the Major Atmospheric Gamma Imaging Cherenkov (MAGIC) telescopes (Mirzoyan 2017). VHE observations by the High-Altitude Water Cherenkov (HAWC; Martinez et al. 2017) Observatory, High Energy Stereoscopic System (HESS; de Naurois 2017), and an initial observation from the Very Energetic Radiation Imaging Telescope Array System (VERITAS; Mukherjee 2017), taken within two weeks of the event as part of its neutrino follow-up program (Santander et al. 2017), did not yield detections. Details of the neutrino detection, the multiwavelength follow-up campaign, and the statistical significance of the neutrino-blazar chance correlation are presented in IceCube Collaboration et al. (2018). While potential counterparts to neutrino events have been proposed in the past (Kadler et al. 2016; Lucarelli et al. 2017), none had previously been detected in the VHE range.

The potential association with an astrophysical neutrino event made TXS 0506+056 a source of particular interest, and further studies of its high-energy emission are required to explore the possible physical connection between the neutrino and gamma-ray emissions. For this purpose, VERITAS performed observations of the blazar between 2017 September and 2018 February, which are presented here.

[27] https://gcn.gsfc.nasa.gov/

[28] https://gcn.gsfc.nasa.gov/notices_amon/50579430_130033.amon

2. Observations and Data Analysis

2.1. VERITAS Observations

VERITAS (Holder et al. 2006) is an instrument dedicated to VHE gamma-ray astrophysics with sensitivity in the 80 GeV to 30 TeV energy range. It consists of an array of four 12 m imaging atmospheric Cherenkov telescopes located at the Fred Lawrence Whipple Observatory in southern Arizona, USA. In its current configuration, VERITAS is able to detect a source with a flux of 1% of the gamma-ray flux of the Crab Nebula within 25 hr of observation (Park et al. 2015).

VERITAS observations of the TXS 0506+056 location were started on 2017 September 23 (MJD 58019.38) in response to the IceCube alert IC 170922A and continued following the *Fermi*-LAT report of flaring activity from the blazar and the detection in VHE gamma-rays by the MAGIC collaboration. A total exposure of 34.9 hr of quality-selected data was accumulated between 2017 September 23 and 2018 February 6 (MJD 58019-58155) with an average zenith angle of 29°. Observations were performed using the standard "wobble" observation mode (Fomin et al. 1994) with a $0.^{\circ}5$ offset in each of four cardinal directions.

The data were analyzed using the standard VERITAS analysis tools (Cogan 2007; Maier & Holder 2017), with background-rejection cuts optimized for soft-spectrum sources (photon index ∼4, Krause et al. 2017). The analysis yields a detection of the source above 110 GeV with a statistical significance of 5.8σ following Equation (17) of Li & Ma (1983), with 1270 events in the ON region, 10,647 events in the OFF region, and a background normalization $\alpha = 0.1$, resulting in a photon excess of 205 events in the ON region. A sky map of statistical significance is shown in Figure 1. The centroid of the gamma-ray excess was determined by fitting the uncorrelated excess counts map with a two-dimensional Gaussian function. The centroid position in J2000 coordinates is R.A. = $77.^{\circ}354$ (or $5^{h}\ 9^{m}\ 25^{s}$), and decl. = $5.^{\circ}702$ (or $5°42'9''$), in good agreement with the Very Long Baseline Array (VLBA) radio position of TXS 0506 +056 (Lanyi et al. 2010) given statistical and systematic uncertainties on each of the centroid coordinates of $0.^{\circ}01$ and $0.^{\circ}007$, respectively. We name the new VERITAS source VER J0509+057.

A differential photon spectrum, shown in Figure 2, was constructed using 10 bins per energy decade in the VHE range. A power law of the form $F(E) = N_0\ (E/E_0)^{-\Gamma}$ fit to the differential spectrum gives a best-fit flux normalization of $N_0 = (6.4 \pm 1.6) \times 10^{-11}\,\mathrm{cm^{-2}\,s^{-1}\ TeV^{-1}}$ at an energy of $E_0 = 0.15$ TeV and a spectral index $\Gamma = 4.8 \pm 1.3$, with a χ^2/n.d.f. of 0.5/1. The integral flux above 110 GeV is $(8.9 \pm 1.6) \times 10^{-12}\,\mathrm{cm^{-2}\,s^{-1}}$, which corresponds to 1.6% of the Crab Nebula flux (Hillas et al. 1998) above the same energy threshold. The average spectrum measured by VERITAS between 2017 September and 2018 February has a flux of ∼60% of that reported by MAGIC in observations obtained within two weeks of the IC 170922A detection (IceCube Collaboration et al. 2018). The spectral indices are consistent given the large statistical uncertainties ($\Gamma_{\mathrm{VERITAS}} = 4.8 \pm 1.3$ and $\Gamma_{\mathrm{MAGIC}} = 3.9 \pm 0.4$). Monte-Carlo simulations indicate that the systematic uncertainty on the VERITAS flux

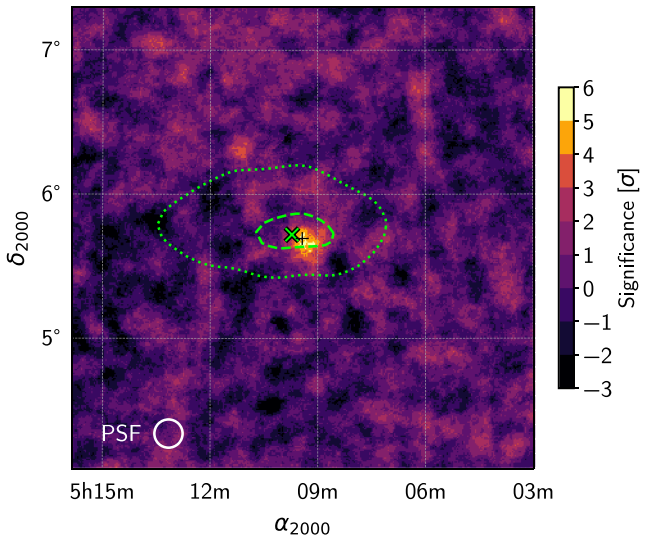

Figure 1. VERITAS statistical-significance sky map for the region around TXS 0506+056. The VLBA radio location of the blazar is indicated with a "+" marker. The size of the VERITAS point-spread function for this analysis, at 68% containment, is shown as a white circle in the lower left. The "x" marker indicates the best-fit position of IC 170922A, with dashed (dotted) lines indicating the 50% (90%) confidence level regions for the neutrino location (from IceCube Collaboration et al. 2018).

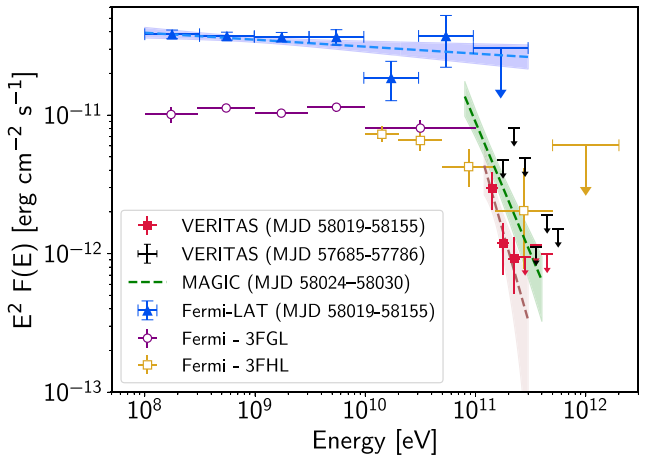

Figure 2. Gamma-ray SED of TXS 0506+056 from *Fermi*-LAT and VERITAS observations collected in the period MJD 58019-58155. Given that the observations are not strictly simultaneous, spectral variability of the source cannot be ruled out. The VHE spectrum of the source as measured by MAGIC within two weeks of the detection of IC 170922A is also shown (IceCube Collaboration et al. 2018). For comparison, the *Fermi*-LAT 3FGL (purple) and 3FHL (orange) catalog fluxes of the source are shown, as well as 95% confidence level (CL) upper limits from VERITAS archival observations (black) described in Section 2.1. Best-fit power laws are shown as dashed lines for each data set collected in the MJD 58019-58155 period, with color bands indicating 68% statistical uncertainties on the fit.

normalization and photon index for a soft-spectrum source like TXS 0506+056 are ∼60% and 0.3, respectively (Abeysekara et al. 2015).

A VERITAS light curve of the integral photon flux above an energy threshold of 110 GeV is shown in Figure 3. For its calculation, the spectral index has been kept fixed at 4.8. Both in the case of the light curve and the differential spectrum, flux points are shown if the significance of the photon excess in the bin is larger than 2σ; otherwise a 95% CL upper limit is calculated using the method of Rolke & López (2001).

Due to its hard GeV-band spectrum, TXS 0506+056 was identified as a promising VHE source candidate and observed by VERITAS prior to the detection of IC 170922A, between 2016 October 10 (MJD 57685) and 2017 February 2 (MJD 57786). No significant gamma-ray excess was found in an analysis of 2.1 hr of quality-selected data collected on the source during this period. A 95% CL integral flux upper limit of $1.2 \times 10^{-11}\,\mathrm{cm^{-2}\,s^{-1}}$ above an energy threshold of 110 GeV was derived at the source location for a spectral index of 4.8, corresponding to 2.1% of the Crab Nebula flux above the same threshold. Differential spectral upper limits computed at the 95% CL are shown in Figure 2 which, given the short exposure, are consistent with the VHE spectrum of the source measured after IC 170922A.

2.2. *Fermi*-LAT Observations

In order to characterize the GeV energy spectrum of the source during the period of VERITAS observations, we perform a power-law fit to data from the *Fermi*-LAT (Atwood et al. 2009) recorded between MJD 58019.38 and 58155.20. The analysis presented here was performed using version `v10r0p5` of the *Fermi* `Science Tools`.[29] Photons with energies between 100 MeV and 300 GeV that were detected within 15° of the location of TXS 0506+056 were selected for the analysis, while photons with a zenith angle larger than 100° were discarded to reduce contamination from the Earth's albedo. The contribution from isotropic and Galactic diffuse backgrounds, and sources in the 3FGL catalog (Acero et al. 2015) within 15° of the source position, were included in the spectral fit with their spectral parameters fixed to their catalog values, while the parameters for sources within 3° were allowed to vary freely during the source spectral fit. The blazar spectral fit was performed with a binned-likelihood method using the `P8R2_SOURCE_V6` instrument response functions.

TXS 0506+056 is strongly detected during the analyzed period, with a test-statistic (TS) of more than 2100 from the *Fermi*-LAT analysis. The power-law best-fit spectral parameters are a photon index $\Gamma = 2.05 \pm 0.03$ (consistent with the 3FGL value of 2.04 ± 0.03) and a flux normalization $N_0 = (1.04 \pm 0.05) \times 10^{-11}\,\mathrm{cm^{-2}\,s^{-1}\,MeV^{-1}}$ at an energy E_0 of 1.44 GeV, about a factor of three higher than the 3FGL value of $(3.24 \pm 0.10) \times 10^{-12}$ in the same units. The spectral fit was repeated in seven independent energy bins with equal logarithmic spacing in the 0.1–300 GeV range. Best-fit flux values and 68% uncertainties, shown in Figure 2, are reported for spectral bins with a TS larger than 4. Flux upper limits at 95% CL are quoted otherwise.

We compute a light curve of integral photon flux between 0.1 and 300 GeV based on the *Fermi*-LAT data binned in seven-day intervals. The integral flux is calculated by fitting the spectrum of the source with a power-law function for each time bin, while allowing the spectral index Γ_{LAT} to vary freely. The integral flux points, all with a TS larger than 9, are shown in Figure 3. For comparison, the integral photon flux in the same energy range is $(2.33 \pm 0.14) \times 10^{-7}\,\mathrm{cm^{-2}\,s^{-1}}$ for the entire period. We characterize the variability of the source in the *Fermi*-LAT band by evaluating the goodness-of-fit of a constant value to the light curve. The flux light curve is poorly fit by a constant, with a χ^2/n.d.f. of 69.4/19 ($p = 1.2 \times 10^{-7}$),

[29] The *Fermi* `Science Tools` can be downloaded from https://fermi.gsfc.nasa.gov/ssc/data/analysis/software/.

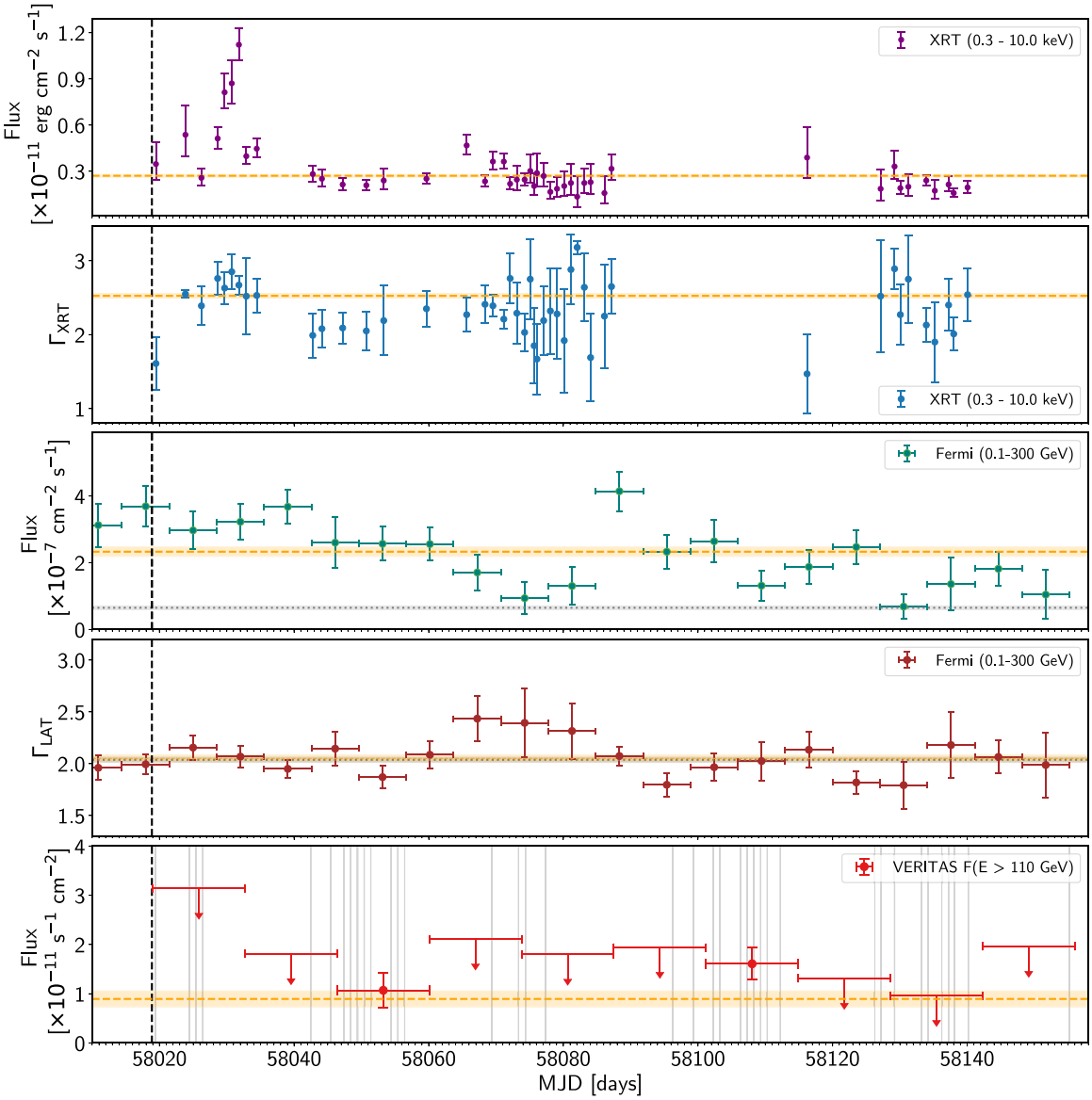

Figure 3. Multiwavelength light curves for TXS 0506+056 derived from *Swift*, *Fermi*-LAT, and VERITAS observations. The dashed vertical line shows the time of detection of the IC 170922A neutrino event. In each panel, the horizontal dashed line and band indicate the mean and 1σ uncertainty of each parameter for the entire period. The catalog flux and spectral index values, and their uncertainties, are shown as gray lines and bands in the *Fermi*-LAT panels. The VERITAS light curve is shown using 10 bins, where each point represents the average flux level of the source during the VERITAS observations collected in that period (shown as vertical gray bands). The upper limits and flux points do not constrain the potential variability of the source during periods in which VERITAS was not observing the blazar.

which confirms the presence of GeV flux variability in the time period considered. For the spectral index, a constant fit yields a χ^2/n.d.f. of 23.9/19 ($p = 0.2$), indicating that a constant index is consistent with the data given the statistical uncertainties.

2.3. *Swift* X-Ray Telescope (XRT) Observations

Prompt follow-up observations of the neutrino error region and later observations of TXS 0506+056 were performed as part of an existing neutrino follow-up program (Evans et al. 2015) using the X-ray Telescope (XRT) on board the Neil Gehrels *Swift* Observatory (Gehrels 2004). Preliminary results from this follow-up were reported by Keivani et al. (2017). A total of 45 *Swift* XRT observations performed during the MJD 58019-58155 period resulted in a total exposure of 74 ks, which we use to characterize the X-ray variability of the source. The observations were conducted in photon-counting mode, with negligible pile-up effects. The data were reduced and calibrated using HEAsoft, XSpec version 12.9.1. The data from each observation (typically ∼1 ks) were fitted with an absorbed power-law spectrum using a Galactic column density of $1.1 \times 10^{21}\,\mathrm{cm}^{-2}$ from the Leiden/Argentine/Bonn (LAB) neutral hydrogen survey (Kalberla et al. 2005) and using `cstat` within XSpec. A good fit was obtained for all observations considered.

The de-absorbed integral photon fluxes and indices in the 0.3–10 keV band from the individual fits are shown in the light curve in Figure 3. The flux is clearly variable during the period both in amplitude and spectral index, with a strong X-ray flare detected in the period MJD 58030-58032 peaking at a flux about four times the time-average for the period, which is $(2.7 \pm 0.1) \times 10^{-12}\,\mathrm{erg\,cm^{-2}\,s^{-2}}$. The time-averaged photon index in XRT was 2.52 ± 0.03.

As in the *Fermi*-LAT case, a quantitative assessment of the flux variability was performed by fitting a constant value to the flux and index curves, both resulting in poor fits (χ^2/ndf of 213/44 and 118/44, respectively) indicating source variability.

3. Discussion

Our analysis indicates that during this period the blazar was about three times brighter in the LAT band compared to its 3FGL value and, while there was significant GeV photon flux variability, the photon index remained consistent with a constant value at the 3FGL level. At the same time, the flux observed by VERITAS is consistent with that reported in a similar energy range in the *Fermi*-LAT 3FHL catalog (Ajello et al. 2017). This could imply that the VERITAS detection is associated with a baseline VHE flux of the source rather than with flaring episodes. As the VERITAS light curve upper limits are consistent with the average flux for the entire period, this hypothesis cannot be ruled out using these data alone. While the variability detected in the LAT and XRT bands has no clear counterpart in the VHE band, the upper limits set by VERITAS are still consistent with a linear scaling of the VHE flux by the same amount as the flux increase observed at lower energies during the active periods, with the additional caveat that the VERITAS observations are not strictly simultaneous with those of XRT and LAT.

The gamma-ray SED in Figure 2 shows a sharp spectral break between the *Fermi*-LAT and VERITAS energy bands during the MJD 58019-58155 period. Although not as pronounced, some spectral curvature is also evident in the flux points reported in the 3FGL and 3FHL catalogs shown in the same figure. This softening is noticeable in the power-law indices reported in *Fermi*-LAT catalogs, which increase with energy threshold ($\Gamma_{\rm 3FGL} = 2.04 \pm 0.03$ for $E > 100$ MeV, $\Gamma_{\rm 3FHL} = 2.16 \pm 0.21$ for $E > 10$ GeV, and $\Gamma_{\rm 2FHL} = 2.76 \pm 0.57$ for $E > 50$ GeV), although with significant uncertainties.

To characterize the intrinsic break we correct the VERITAS and *Fermi*-LAT flux points for extragalactic background light (EBL) absorption using the model of Franceschini et al. (2008) and the source redshift of $z = 0.3365 \pm 0.0010$ (Paiano et al. 2018), and perform a joint fit of the gamma-ray spectrum. The SED is well-described using a power-law function with exponential cutoff of the form $N_0(E/E_0)^{-\Gamma}\exp(-E/E_c)$. For a normalization energy E_0 of 1.44 GeV the best-fit parameters are $N_0 = (1.12 \pm 0.05) \times 10^{-8}\,{\rm cm}^{-2}\,{\rm s}^{-1}\,{\rm GeV}^{-1}$, $E_c = 63 \pm 7$ GeV, and $\Gamma = 2.02 \pm 0.03$, with a χ^2/n.d.f. of 6.05/6 ($p = 0.42$). The de-absorbed spectrum and best-fit solution are shown in Figure 4. This result indicates that the break cannot be attributed to EBL absorption of a power-law spectrum alone, as illustrated by the extrapolation of the *Fermi*-LAT power-law spectrum to VHE energies, which fails to fit the VERITAS observations after accounting for EBL absorption. If the blazar is the source of the neutrino, the paucity of high-energy emission may imply that the hadronic gamma-ray emission is strongly attenuated at the source, and potentially cascades down to energies lower than the *Fermi*-LAT band (Murase et al. 2016; Gao et al. 2017). The soft XRT photon index and lower XRT energy flux compared to the >100 MeV band places the X-ray emission in the first SED bump, pushing any potential cascaded emission to the hard X-ray MeV band. Future measurements of the "valley" between the SED bumps will be crucial in constraining the contribution to the SED of potential neutrino counterparts from cascaded emission.

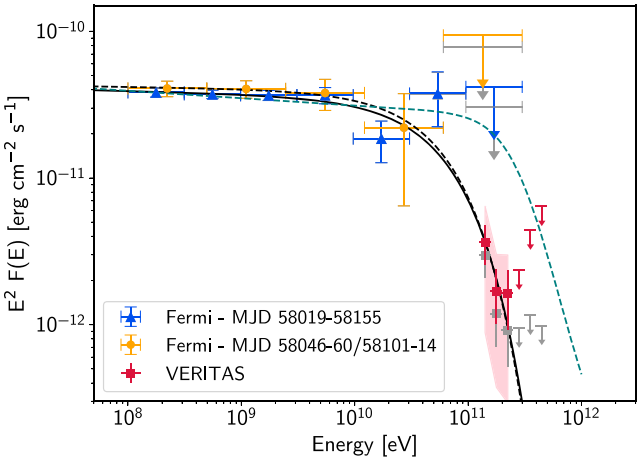

Figure 4. Power-law fit with an exponential cutoff to the de-absorbed gamma-ray SED of TXS 0506+056 using *Fermi*-LAT data from the period MJD 58019-58155 (solid black line) and MJD 58046-60/58101-58114 (dashed black line). De-absorbed flux points are shown in color, and observed fluxes in gray. The teal dashed line shows an extrapolation of the *Fermi*-LAT fit from Section 2.2 to VHE energies that accounts for EBL absorption using the model of Franceschini et al. (2008). The pink band in the VHE range illustrates the energy-scale systematic uncertainty on the VERITAS spectrum.

The sharpness of the break may be sensitive to relative flux variations between the *Fermi*-LAT and VERITAS bands as the observations are not strictly simultaneous. As shown in Figure 3, most of the VERITAS signal is collected during two time periods: MJD 58046-60 and 58101-58114. We obtained a second *Fermi*-LAT spectrum, also shown in Figure 4, by restricting the analysis to this period and repeating the SED fit that yields best-fit parameters of $N_0 = (1.2 \pm 0.1) \times 10^{-8}\,{\rm cm}^{-2}\,{\rm s}^{-1}\,{\rm GeV}^{-1}$, $E_c = 61 \pm 11$ GeV, and $\Gamma = 2.01 \pm 0.07$, with a χ^2/n.d.f. of 1.3/4 ($p = 0.86$), consistent with the fit for the entire period. This indicates that the break between both bands is robust to the observed relative flux variability, even after accounting for systematic uncertainties in the VERITAS energy scale (Figure 4).

The detection of TXS 0506+056 in the VHE band during extended follow-up observations of the IC 170922A event represents the first time that such observations have revealed a new VHE gamma-ray source. This detection will inform future neutrino follow-up strategies, as the potential gamma-ray counterparts may be active over time periods of weeks or months, requiring multiple exposures. Continued observations in the future could clarify if blazars are indeed sources of astrophysical neutrinos detected by IceCube.

This research is supported by grants from the U.S. Department of Energy Office of Science, the U.S. National Science Foundation and the Smithsonian Institution, and by NSERC in Canada. We acknowledge the excellent work of the technical support staff at the Fred Lawrence Whipple Observatory and at the collaborating institutions in the construction and operation of the instrument.

This research has made use of publicly available *Fermi*-LAT data and analysis software obtained from the *Fermi* Science Support Center at the High Energy Astrophysics Science Archive Research Center (HEASARC), provided by NASA's Goddard Space Flight Center. This research made use of

Astropy, a community-developed core Python package for Astronomy (Astropy Collaboration et al. 2013); matplotlib, a Python library for publication quality graphics (Hunter 2007); and NumPy (Van Der Walt et al. 2011).

Facilities: VERITAS, *Fermi*-LAT, *Swift*.

ORCID iDs

W. Benbow https://orcid.org/0000-0003-2098-170X
R. Bird https://orcid.org/0000-0002-4596-8563
J. L. Christiansen https://orcid.org/0000-0002-8035-4778
Q. Feng https://orcid.org/0000-0001-6674-4238
J. P. Finley https://orcid.org/0000-0002-8925-1046
A. Furniss https://orcid.org/0000-0003-1614-1273
G. H. Gillanders https://orcid.org/0000-0001-8763-6252
D. Hanna https://orcid.org/0000-0002-8513-5603
C. A. Johnson https://orcid.org/0000-0002-0641-7320
P. Kaaret https://orcid.org/0000-0002-3638-0637
D. Kieda https://orcid.org/0000-0003-4785-0101
M. Krause https://orcid.org/0000-0001-7595-0914
M. J. Lang https://orcid.org/0000-0003-4641-4201
R. Mukherjee https://orcid.org/0000-0002-3223-0754
M. Pohl https://orcid.org/0000-0001-7861-1707
E. Pueschel https://orcid.org/0000-0002-0529-1973
G. T. Richards https://orcid.org/0000-0002-1408-807X
M. Santander https://orcid.org/0000-0001-7297-8217
K. Shahinyan https://orcid.org/0000-0001-5128-4160
D. A. Williams https://orcid.org/0000-0003-2740-9714

References

Aartsen, M. G., Abraham, K., Ackermann, M., et al. 2017, ApJ, 835, 45
Abeysekara, A. U., Archambault, S., Archer, A., et al. 2015, ApJL, 815, L22
Acero, F., Ackermann, M., Ajello, M., et al. 2015, ApJS, 218, 23
Ajello, M., Atwood, W. B., Baldini, L., et al. 2017, ApJS, 232, 18
Astropy Collaboration, Robitaille, T. P., Tollerud, E. J., et al. 2013, A&A, 558, A33
Atwood, W. B., Abdo, A. A., Ackermann, M., et al. 2009, ApJ, 697, 1071
Böttcher, M., Reimer, A., Sweeney, K., & Prakash, A. 2013, ApJ, 768, 54
Cogan, P. 2007, Proc. ICRC (Merida), 3, 1385, arXiv:0709.4233
de Naurois, M. 2017, ATel, 10787, 1
Dermer, C. D., & Giebels, B. 2016, CRPhy, 17, 594
Evans, P. A., Osborne, J. P., Kennea, J. A., et al. 2015, MNRAS, 448, 2210
Fomin, V. P., Stepanian, A. A., Lamb, R. C., et al. 1994, APh, 2, 137
Franceschini, A., Rodighiero, G., & Vaccari, M. 2008, A&A, 487, 837
Gao, S., Pohl, M., & Winter, W. 2017, ApJ, 843, 109
Gehrels, N. 2004, in AIP Conf. Ser. 727, Gamma-Ray Bursts: 30 Years of Discovery, ed. E. E. Fenimore & M. Galassi (Melville, NY: AIP), 637
Halzen, F., & Zas, E. 1997, ApJ, 488, 669
Hillas, A. M., Akerlof, C. W., Biller, S. D., et al. 1998, ApJ, 503, 744
Holder, J., Atkins, R., Badran, H., et al. 2006, APh, 25, 391
Hunter, J. D. 2007, CSE, 9, 90
IceCube Collaboration 2013, Sci, 342, 1242856
IceCube Collaboration et al. 2018, Sci, submitted, doi:10.1126/science.aat1378
Kadler, M., Krauß, F., Mannheim, K., et al. 2016, NatPh, 12, 807
Kalberla, P. M. W., Burton, W. B., Hartmann, D., et al. 2005, A&A, 440, 775
Keivani, A., Evans, P. A., Kennea, J. A., et al. 2017, ATel, 10792, 1
Kopper, C., & Blaufuss, E. 2017, GCN, 21916, 1
Krause, M., Pueschel, E., & Maier, G. 2017, APh, 89, 1
Lanyi, G. E., Boboltz, D. A., Charlot, P., et al. 2010, AJ, 139, 1695
Li, T.-P., & Ma, Y.-Q. 1983, ApJ, 272, 317
Lucarelli, F., Pittori, C., Verrecchia, F., et al. 2017, ApJ, 846, 121
Madejski, G., & Sikora, M. 2016, ARA&A, 54, 725
Maier, G., & Holder, J. 2017, Proc. ICRC (Busan), arXiv:1708.04048
Mannheim, K. 1993, A&A, 269, 67
Mannheim, K. 1995, APh, 3, 295
Martinez, I., Taboada, I., Hui, M., & Lauer, R. 2017, ATel, 10802, 1
Mirzoyan, R. 2017, ATel, 10817, 1
Mukherjee, R. 2017, ATel, 10833, 1
Murase, K., Guetta, D., & Ahlers, M. 2016, PhRvL, 116, 071101
Paiano, S., Falomo, R., Treves, A., & Scarpa, R. 2018, ApJL, 854, L32
Park, N., et al. 2015, Proc. ICRC (The Hague), 34, 771
Rolke, W. A., & López, A. M. 2001, NIMPA, 458, 745
Santander, M., Dorner, D., Dumm, J., et al. 2017, Proc. ICRC (Busan), arXiv:1708.08945
Smith, M. W. E., Fox, D. B., Cowen, D. F., et al. 2013, APh, 45, 56
Tanaka, Y. T., Buson, S., & Kocevski, D. 2017, ATel, 10791, 1
Van Der Walt, S., Colbert, S. C., & Varoquaux, G. 2011, CSE, 13, 22